Applied Catalysis B: Environmental 92 (2009) 240–249

Contents lists available at ScienceDirect

Applied Catalysis B: Environmental

journal homepage: www.elsevier.com/locate/apcatb

# Photocatalytic degradation of organics in water in the presence of iron oxides: Influence of carboxylic acids

Eva Rodríguez, Guadalupe Fernández, Beatriz Ledesma, Pedro Álvarez, Fernando J. Beltrán *

*Departamento de Ingeniería Química y Química Física, Universidad de Extremadura, 06071 Badajoz, Spain*

ARTICLE INFO

*Article history:*
Received 27 April 2009
Received in revised form 3 July 2009
Accepted 15 July 2009
Available online 22 July 2009

*Keywords:*
Bisphenol A
Photocatalytic oxidation
Iron oxides
Hematite
Magnetite
Carboxylic acids
Titania
Hydrogen peroxide

ABSTRACT

The effects of four carboxylic acids: malic, citric, tartaric and oxalic acids on the leaching of iron from two commercial iron oxides (hematite, $\alpha$-$Fe_2O_3$, and magnetite, $Fe_3O_4$) have been investigated. The variables studied were the doses of iron oxides and carboxylic acids used as well as aqueous pH, temperature and the presence of hydrogen peroxide and/or UV-A radiation. On the whole, $Fe_3O_4$ led to higher amounts of leached iron than $\alpha$-$Fe_2O_3$, and oxalic acid was the most effective carboxylic acid used. The importance of iron leaching has been considered to explain the photodegradation of bisphenol A (BPA) by UV-A/iron oxides systems. The influence of the presence of hydrogen peroxide and/or titania on the efficiency of these oxidation systems was also investigated. At the conditions tested, advanced oxidation with the UV-A/iron oxide/oxalic acid/$H_2O_2$/$TiO_2$ system led to the lowest BPA half life (<15 min) among those processes studied.

© 2009 Elsevier B.V. All rights reserved.

## 1. Introduction

Nowadays the presence in the water environment of many synthetic organic chemicals able to alter living being endocrine systems is a subject of great concern [1]. Removal of this kind of contaminants from water is compulsory and only tertiary treatment methods such as membrane technologies, adsorption or advanced chemical oxidation fulfill this task. Among these technologies, only advanced oxidation processes (AOPs) destroy the contaminants. AOPs are characterized for the production of hydroxyl radicals, very strong oxidizing species that unselectively react with most of the contaminants in water [2]. AOPs based on the simultaneous use of radiation and semiconductors have attracted the interest of many researchers [3,4]. In particular, the combination of UV-A radiation and titania constitutes one of the most studied advanced photochemical oxidation technologies [5,6]. Another interesting photocatalytic oxidation process is the combination of UV-A radiation and iron, just dissolved or as oxides. The efficiency of this oxidizing system can be improved by the presence of some carboxylic acids that in the presence of iron form carboxylate complexes that absorb UV-A radiation with high quantum yield to trigger radical chain mechanisms of oxidation [7–10]. Literature reports some works on the removal of contaminants with UV-A radiation/iron/carboxylate oxidation systems. Thus, oxalic, citric and tartaric acids have been used with UV-A/Fe(III) to improve the removal of contaminants such as dyes, herbicides, benzene, etc., through the formation and photodecomposition of iron–carboxylate complexes that improve the generation of oxidizing free radicals [11–14]. These processes are of great interest since carboxylic acids, such as oxalic acid, are usually intermediate or end products of the hydroxyl radical oxidation of organic contaminants in water [15]. Also, the use of iron oxides as photocatalysts is recommended due to their abundance on earth. In fact, literature reports some recent works where compounds such as bisphenol A, 2-mercaptobenzothiazol and pentachlorophenol are removed from water with these oxidizing systems [16–19]. However, when using iron oxides and carboxylic acids to photocatalytically remove contaminants from water, studies on iron leaching into water are also needed due to the importance of dissolved iron–carboxylic acids complexes on the process performance.

Main factors affecting iron oxide dissolution are the properties of the overall system (temperature, UV light), the composition of the solution phase (pH, redox potential, concentration of acids, reductants and complexing agents) and the properties of the oxide (specific surface area, stoichiometry, crystal chemistry, crystal defects or guest ions). However, only the composition of the solution and the tendency of ions in solution to form complexes were considered important in mechanistic studies [20,21]. Iron oxide dissolution requires the breaking of bonds

* Corresponding author. Tel.: +34 924 289 387; fax: +34 924 289 385.
*E-mail address:* fbeltran@unex.es (F.J. Beltrán).

0926-3373/$ – see front matter © 2009 Elsevier B.V. All rights reserved.
doi:10.1016/j.apcatb.2009.07.013

between surface Fe(III) and lattice neighbors (e.g., lattice oxygen). Surface chemical processes that weaken these bonds such as protonation of surface sites, adsorption of ligands, and (photo)-reduction of surface sites by reductive agents all lead to polarization of metal–oxygen bonds and therefore promote iron oxide dissolution [21–24].

Regarding the dissolution rate, some consistent mineral-specific differences from studies comparing different oxides have evolved. For example, for the most crystalline oxides Sidhu et al. [25] found that the dissolution rate (HCl 0.5 M, 25 °C) follows the order lepidocrite > magnetite > akageneite > maghemite > hematite > goethite. Litter and Blesa [7] compared the dissolution rate of magnetite, maghemite and hematite (EDTA 0.02 M, pH 3, 30 °C) in the presence of UV light or Fe(II). They found that dissolution rate order was magnetite > maghemite ≫ hematite demonstrating the low dissolution ability of the corundum-structure oxides (hematite) compared to that of the spinel-structured oxides and attributing this to higher electron mobility in the spinel structure.

Light-induced dissolution of iron oxides has been subject of many studies [26–35]. This process can be interpreted as a reductive dissolution one and generally involves these steps: (1) Photoexcitation followed by charge transfer resulting in the reduction of surface Fe(III) to Fe(II). (2) Detachment of reduced Fe(II) from the mineral surface. Although different mechanisms can result in the formation of surface Fe(II), irrespective of the mechanism involved, the rate determining step in the dissolution of crystalline iron oxides is generally the detachment of Fe(II) from the mineral surface.

Bisphenols are categorized as one of the main potential endocrine disruptors. Specifically, bisphenol A (BPA), used in many industries to produce polycarbonates, resins, retardants, fungicides, etc., is the prototype of this family of contaminants that has been detected in water due to industrial discharges, landfill leachates and wastewaters containing residues of plastics [36]. Use of AOPs to remove BPA from water has been widely reported, especially for the case of ozonation processes [37]. For the case of UV-A radiation and iron oxides, Li et al. [16,17] report the use of laboratory prepared iron oxides and oxalic acid to improve the oxidation rate.

According to the preceding comments, the main aims of this work were to study the effects of variables such as pH, temperature, presence of other oxidants and light on iron leaching from commercial iron oxides in carboxylic acid aqueous solutions, and the efficiency of the corresponding photocatalytic process on the removal of BPA taken as model contaminant.

## 2. Experimental

### 2.1. Products, experimental set-up and procedure

BPA (4-4′-dihydroxy-2-2-diphenylpropane), citric and malic acids were obtained from Aldrich (Spain), oxalic and perchloric acids from Merck (Spain) and tartaric acid from Riedel-De Häen AG Seles Hannover (Germany). Two iron oxides have been used in this work: a natural red iron oxide and a black synthetic one, both taken from Bendix (Spain). Powdered P25 $TiO_2$ was directly obtained from the manufacturer, Degussa AG (Germany). Two 15 W black light lamps (HQPower Lamp15TBL) emitting mainly 365 nm radiation were used.

Iron leaching experiments were carried out in 125 mL amber borosilicate flasks submerged in a thermostatic bath. In order to investigate the influence of UV-A radiation on the leaching of iron a black lamp was placed at the top of clear borosilicate flasks. In some experiments, mechanical agitation of the reaction mixture was provided.

Photocatalytic BPA oxidation experiments were carried out in a 4 L cylindrical borosilicate glass reactor. The reactor was provided with magnetic agitation, air feeding system and devices for temperature and pH measurements. Two black lamps were installed on opposing walls outside the reactor and the overall system was placed in a closed box to avoid the disturbing effect of direct sunlight irradiation.

Aqueous solutions fed to the flasks and photoreactor were prepared from concentrated standard aqueous solutions of carboxylic acids studied (0.1 and 0.4 M), perchloric acid (3 M) and BPA ($5 \times 10^{-4}$ M) diluted with ultra pure water (Milli Q Millipore Water) to reach the desired concentrations. Perchloric acid or sodium hydroxide was used to fix the pH value.

To start the photocatalytic experiments, 3 L of a buffered BPA aqueous solution ($10^{-5}$ M) pH 3 (perchloric/perchlorate ionic strength 0.03 M) were fed to the reactor, air bubbling was set at 40 L $h^{-1}$ and the lamps were turned on. About 20 min later, time enough to allow the lamps work steadily, desired amounts of iron oxide, carboxylic acid, hydrogen peroxide and/or $TiO_2$ were added. At regular intervals of time, liquid samples were withdrawn from the reactor to be analyzed.

Before BPA analysis some microlitres of sodium thiosulphate were added to eliminate residual oxidants. In all cases, samples were filtered through 0.45 μm PVDF Millipore filters to separate the remaining iron oxide and/or $TiO_2$ particles. Use of Nylon filters was avoided since BPA is retained on them.

### 2.2. Analytical determinations

Textural characterization of iron oxides was accomplished by adsorption of nitrogen at 77 K (Quantachrome Autosorb-1 automated gas adsorption system) and X-ray diffraction (PW-1700 Philips diffractometer with Kα1 Cu radiation and registered $2\theta$ values between 20° and 70°). Specific surface areas of 23 and 26 $m^2\ g^{-1}$ and total pore volume of 0.06 and 0.07 $cm^3\ g^{-1}$ were determined for the natural and synthetic commercial iron oxides, respectively, which suggests non-porous materials with low surface areas and, hence, low capacity for adsorbing organic compounds. X-ray diffractometry, confirmed the nature of the natural red iron oxide and the synthetic black iron oxide as hematite ($\alpha$-$Fe_2O_3$) and magnetite ($Fe_3O_4$), respectively.

BPA concentration was determined by HPLC (Agilent 1100) in a 15 cm long, 0.4 cm i.d. Kromasil C18 column with acetonitrile–water (15/85, v/v) with 0.1% phosphoric acid as mobile phase (flow rate: 1 mL $min^{-1}$). Detection was made at 280 nm. Total iron concentration was determined by the ferrozine method [38] that, briefly, consisted in the reduction to Fe(II) and further formation of a violet complex with the ferrozine reagent (molar absorptivity at 565 nm was 27,044 $M^{-1}\ cm^{-1}$ [39]). In some cases where high oxalic acid concentrations (>0.1 M) were used, the ferrozine reagent was unable to capture all the carboxylic acid from the iron complex and sample dilution was not possible due to the detection limit of the method. Thus, in these cases an AA 140 Varian atomic absorption spectrometer was used to measure total Fe concentration. Fe(II) concentration was determined by the method of Zuo [40] with o-phenantroline by measuring the absorbance at 510 nm of the complex (molar absorptivity: 11,040 $M^{-1}\ cm^{-1}$ [39]). Hydrogen peroxide at concentrations higher than $10^{-3}$ M was iodometrically determined while at lower concentrations the method of Eisenberg [41], based on the 405 nm absorption measurement of a yellow peroxytitanium complex formed, or the Masschelein's method [42] based on the 260 nm measurement of a carbonate–cobaltate(III) complex formed through the hydrogen peroxide oxidation of cobalt and bicarbonate, was applied. The intensity of UV-A radiation coming from the black light lamps into the aqueous solution was obtained by ferrioxalate actinometry

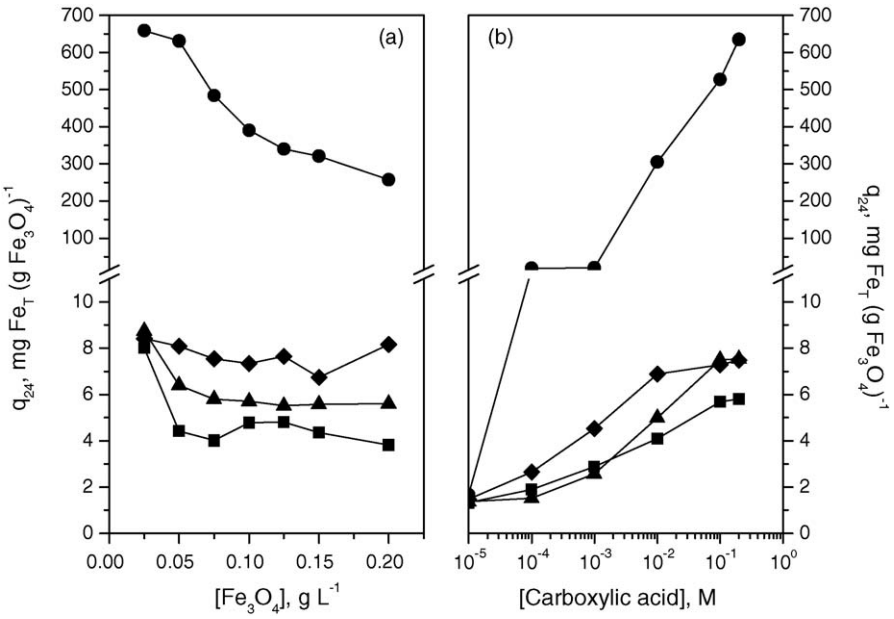


**Fig. 1.** Influence of iron oxide dose (a) and carboxylic acid concentration (b) on $q_{24}$ values for the $Fe_3O_4$/carboxylic acid systems. Experimental conditions: pH 3; 20 °C; No agitation (a): [Carboxylic acid] = 0.01 M; (b): [$Fe_3O_4$] = 0.15 g $L^{-1}$. Symbols: ■ Malic acid; ● Oxalic acid; ▲ Tartaric acid; ◆ Citric acid.

[43]. A photon flow per unit volume of $2.44 \times 10^{-7}$ einstein $s^{-1}$ $L^{-1}$ was determined with both lamps simultaneously working. Total organic carbon was measured with a TOC-$V_{SCH}$ Shimadzu analyzer.

## 3. Results and discussion

### 3.1. Leaching of iron in water

The following variables were studied to investigate their influence on iron leaching: iron oxide and carboxylic acids nature and dose, pH, temperature, agitation speed, presence of hydrogen peroxide and UV-A radiation application.

#### 3.1.1. Iron oxide nature and carboxylic acid effects

Fig. 1 shows the effect of iron oxide doses and carboxylic acids initial concentration on the amount of iron leached from $Fe_3O_4$ after 24 h contact time ($q_{24}$, mg $Fe_T$/g of iron oxide). Qualitatively similar figures were obtained for the case of α-$Fe_2O_3$ (not shown) but the amount of iron leached out from the oxide was always much lower than from $Fe_3O_4$. From Fig. 1 it is apparent that oxalic acid leads to higher amounts of leached iron than any other carboxylic acid used. From Fig. 1a it is observed that the relative amount of iron leached slightly decreases with the increasing iron oxide dose in the presence of carboxylic acids. In Fig. 1b it is shown that the increasing oxalic acid dose applied leads to significant relative iron leached values, the effect for the other carboxylic acids tested being only slightly positive on $q_{24}$. The results obtained indicate the existence of a critical oxalate–iron oxide ratio above which the efficiency of the iron leaching process significantly increases. This ratio was found to be 0.5 and 0.05 mol of oxalate per gram of α-$Fe_2O_3$ and per gram of $Fe_3O_4$, respectively. The structure of the two iron oxides could explain the huge difference observed in the iron leaching efficiency. Thus, the corundum structure (hematite) is more stable than the inverse spinel structure of magnetite [7]. Regardless of the type of iron oxide applied, the iron extraction capacity of the different carboxylic acids tested followed the order malic < tartaric < citric ≪ oxalic acid.

The effect of the different carboxylic acids can be explained taking into account their acidity and their capacity of forming Fe(III)-complexes. Thus, according to the literature, the ideal agent for iron(III) oxides ligand promoted dissolution should be a strong acid of an anion which is a good ligand for Fe(III). A compound that comes close to these requirements is oxalic acid that presents a moderate acid strength (p$K_{a1}$ = 1.25; p$K_{a2}$ = 4.27) and forms Fe(III)-complexes of high stability (being log of stability constants $\beta_1$ = 7.53; $\beta_2$ = 13.64 and $\beta_3$ = 18.49) [[44,45] and references there in].

In these cases, the reaction for ligand promoted dissolution may be written as follows [23,24]:

$$\equiv \mathrm{Fe(III)} - \mathrm{OH}^{+} + \mathrm{L}^{n-} + \mathrm{H}^{+} \rightarrow [\equiv \mathrm{Fe(III)} - \mathrm{L}]^{(n-2)-} + \mathrm{H_2O} \quad (1)$$

#### 3.1.2. Effect of aqueous pH

The effect of this variable is shown in Fig. 2 for the case of $Fe_3O_4$. From Fig. 2 it is observed that the increasing pH yields to decreasing values of $q_{24}$, the results with oxalic acid being the most significant. In all cases, iron leaching is nearly negligible at neutral pH. A similar tendency was observed when α-$Fe_2O_3$ was used,

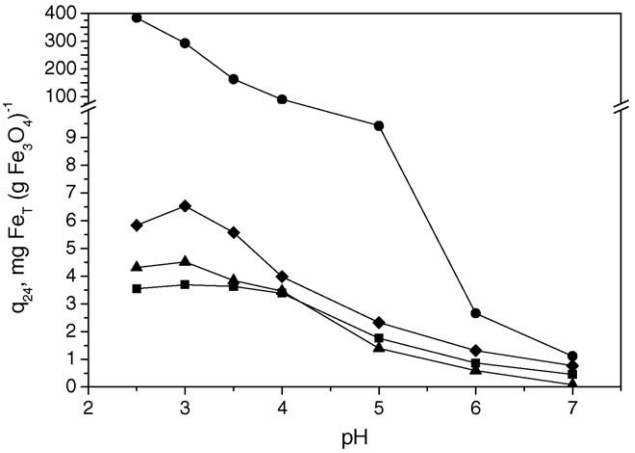


**Fig. 2.** Influence of pH on $q_{24}$ values for the $Fe_3O_4$/carboxylic acid systems. Experimental conditions: 20 °C; No agitation. [Carboxylic acid] = 0.01 M; [$Fe_3O_4$] = 0.15 g $L^{-1}$. Symbols: ■ Malic acid; ● Oxalic acid; ▲ Tartaric acid; ◆ Citric acid.

being $q_{24} < 1$ mg g$^{-1}$ for all the carboxylic acids tested at pH > 4 at the experimental conditions applied in this work, being these results coincident with others from previous works [24,43,44]. From the results obtained it was also observed that the increase in contact time (not shown) leads to increases in iron leaching, regardless of the carboxylic acid and iron oxide used and working pH. Thus, after 72 h contact time at pH 2.5 with 0.01 M oxalic acid and 0.15 g L$^{-1}$ iron oxide, the relative amount of iron leached from $Fe_3O_4$ was 663 mg g$^{-1}$ (see also $q_{24}$ values in Fig. 1a when working with 0.01 M oxalic acid and 0.025 g L$^{-1}$ $Fe_3O_4$ at pH 3 and, in Fig. 1b, with 0.2 M oxalic acid and 0.15 g L$^{-1}$ $Fe_3O_4$ at pH 3), close to 723 mg g$^{-1}$ that corresponds to the theoretical value, calculated in accordance with the chemical formulae of the oxide (assuming 100% iron oxide purity). At the same conditions, the amount of iron leached from α-$Fe_2O_3$ was always less than 20 mg g$^{-1}$, far from the theoretical value (700 mg g$^{-1}$).

### 3.1.3. Effect of temperature

Fig. 3 shows the changes of $q$ versus time when working with 0.15 g L$^{-1}$ of the iron oxide in the presence of 0.01 M oxalic acid at pH 3 and different temperatures. As expected [24,44,46,47], temperature has a clear positive effect on iron leaching from both oxides, but when $Fe_3O_4$ is at temperatures higher than 30 °C the process seems to be mass transfer controlled. This mass transfer effect was also observed for the $Fe_3O_4$–tartaric acid system at 20–40 °C although in this case $q_{24}$ values were lower than 20 mg g$^{-1}$.

### 3.1.4. Effect of agitation speed

Samples containing iron oxides and carboxylic acids were also subjected to 800 rpm agitation and the results compared to those obtained at no agitation conditions. Fig. 4 shows the effect of this variable on iron leaching from the $Fe_3O_4$. As it is observed from Fig. 4 agitation speed has no influence at all when carboxylic acids different than oxalic acid are present in solution. Thus, at the conditions applied in this study mass transfer is not the controlling step of the iron leaching rate. However, for the oxalic acid/$Fe_3O_4$ system a positive effect of agitation is observed, that is, mass transfer controls, at least partially, the leaching process rate. For the carboxylic acid/α-$Fe_2O_3$ systems at room temperature agitation speed caused no effect on iron leaching regardless of the carboxylic acid tested and agitation speed, which suggests surface chemical reactions control the leaching process rate.

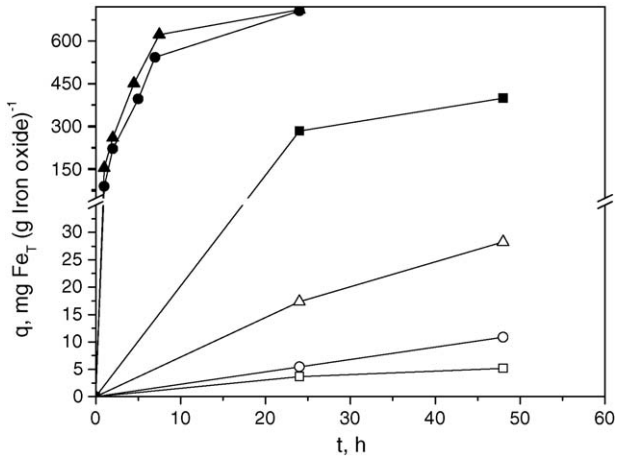


**Fig. 3.** Influence of temperature on $q$ changes with time for the α-$Fe_2O_3$/oxalic acid (open symbols) and $Fe_3O_4$/oxalic acid (solid symbols) systems. Experimental conditions: pH 3; No agitation. [Oxalic acid] = 0.01 M; [Iron oxide] = 0.15 g L$^{-1}$. Symbols: ■, □ 20 °C; ●, ○ 30 °C; ▲, △ 40 °C.

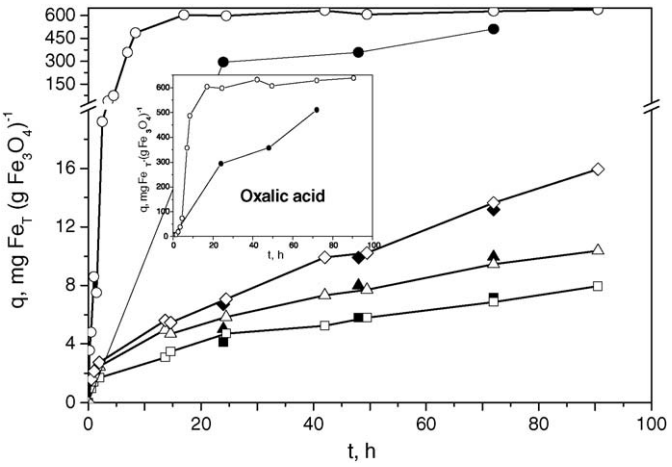


**Fig. 4.** Influence of agitation speed on $q$ changes with time for the $Fe_3O_4$/carboxylic acid systems. Experimental conditions: pH 3; 20 °C; [Carboxylic acid] = 0.01 M; [$Fe_3O_4$] = 0.15 g L$^{-1}$. Symbols (solid: agitation speed 0 rpm; open: agitation speed 800 rpm): ■, □ Malic acid; ●, ○ Oxalic acid; ▲, △ Tartaric acid; ◆, ◇ Citric acid.

### 3.1.5. Effect of hydrogen peroxide

Some authors have pointed out that during the leaching process, Fe(III) reduces to Fe(II) on the oxide surface due to electron transfer from the adsorbed carboxylic acid [23]. Fe(II) also forms complexes with carboxylates so they can be formed on the oxide surface and diffuse into the bulk water catalyzing the leaching process.

The reduction of structural Fe(III) to Fe(II) destabilizes the coordination sphere of the iron both as a result of the loss of charge and because of the larger size of the Fe(II) and thus induces detachment of iron as Fe(II). Examples of reductants are dithionite, ascorbic acid, sucrose, thyoglycolic acid, hydroquinone and the Fe(II) ion [21].

Also Fe(II) ions accelerate the reductive dissolution of iron oxides. Fe(II) ions when present in the solid iron oxide network, can be transferred to the water. In the absence of Fe(II) ions on the iron oxide network, appearance of these ions on solution in the presence of some ligand can be explained by the following Fe(III) reduction reaction [23,24]:

$$[\equiv \mathrm{Fe(III)} - \mathrm{L}]^{(n-2)-} \rightleftarrows \mathrm{Fe(II)_{aq}} + \text{product of ligand oxidation} \quad (2)$$

$$\mathrm{Fe(II)_{aq}} + \mathrm{L}^{n-} \rightarrow [\mathrm{Fe(II)} - \mathrm{L}]_{\mathrm{aq}}^{(n-2)-} \quad (3)$$

Thus, in order to ascertain whether a reductive or non-reductive dissolution takes place when the iron oxides are in contact with the different carboxylic acids, in some experiments the concentration of Fe(II) was tried to be measured. However, in no case, Fe(II) was detected. Similar results have been obtained by Xu and Gao [47] when studying hematite dissolution in the presence of oxalate. These authors reported the absence of reductive dissolution of the iron oxide in the presence of oxalic acid. Taxiarchou et al. [24] proposed that in an oxygen saturated media at pH 3 dissolved Fe(II) rapidly oxidizes to Fe(III). In this work, Fe(II) formation was tried to be checked by adding hydrogen peroxide to some experiments. It was expected hydrogen peroxide would compete with dissolved oxygen to oxidize Fe(II), if present in water, through the well-known Fenton reaction [48]:

$$\mathrm{Fe(II)} + \mathrm{H_2O_2} \rightarrow \mathrm{Fe(III)} + \mathrm{HO^{\bullet}} + \mathrm{HO^-} \quad (4)$$

Hence, a decrease in hydrogen peroxide concentration should be observed if, during the leaching process, Fe(III) is reduced to Fe(II). From these experiments (0.15 g L$^{-1}$ iron oxide, absence of carboxylic acid or 0.01 M carboxylic acid, $5 \times 10^{-4}$ M hydrogen

peroxide, pH 3, 20 °C and 800 rpm) no changes in hydrogen peroxide concentration were observed in the absence of carboxylic acids or when oxalic, malic and citric acids were used, but a significant decrease in hydrogen peroxide concentration was noticed in the presence of tartaric acid and any of the iron oxides used (results not shown). In iron oxides free experiments the presence of the carboxylic acids did not affect the concentration of hydrogen peroxide. On the other hand, at the experimental conditions of this work, the amount of iron leached from both iron oxides was not dependent on the hydrogen peroxide present in the water. According to these results, for the iron oxide/tartaric acid system a reductive dissolution of both iron oxides takes place and a Fe(II)–tartaric acid complex is formed that is rapidly oxidized (in the bulk and/or in the iron oxide surface) to Fe(III) through the Fenton reaction (Eq. (4)). For the case of iron oxides/malic or citric or oxalic acid systems, results would indicate that neither Fe(II)-complex is leached to the water nor formed on the iron oxide surface.

Finally, in order to establish if hydroxyl radicals could be formed through the reaction of hydrogen peroxide with structural Fe(II) or Fe(III) present on the oxide surface, that is, through an apparent heterogeneous Fenton reaction [49–56], two new experiments were carried out in the absence of carboxylic acids (0.15 g $L^{-1}$ iron oxide, $5 \times 10^{-4}$ M hydrogen peroxide, pH 3, 20 °C and 800 rpm) with BPA ($10^{-5}$ M) as hydroxyl radical probe compound. Lin and Gurol [49], from their results on hydrogen peroxide decomposition in the presence of goethite (α-FeOOH), reported the following simplified mechanism of reactions on the iron surface:

$$\equiv \mathrm{Fe(III)} - \mathrm{OH} + \mathrm{H_2O_2} \rightleftharpoons (\mathrm{H_2O_2})_s \quad (5)$$

$$(\mathrm{H_2O_2})_s \rightarrow \equiv \mathrm{Fe(II)} + \mathrm{H_2O} + \mathrm{HO_2^\bullet} \quad (6)$$

$$\equiv \mathrm{Fe(II)} + \mathrm{H_2O_2} \rightarrow \equiv \mathrm{Fe(III)} - \mathrm{OH} + \mathrm{HO^\bullet} \quad (7)$$

$$\mathrm{HO_2^\bullet} \rightleftharpoons \mathrm{H^+} + \mathrm{O_2^{\bullet -}} \quad (\mathrm{p}K_a = 4.8) \quad (8)$$

$$\equiv \mathrm{Fe(III)} - \mathrm{OH} + \mathrm{HO_2^\bullet} \rightarrow \equiv \mathrm{Fe(II)} + \mathrm{H_2O/OH^-} + \mathrm{O_2} \quad (9)$$

If only structural Fe(III) is present (as it would be expected in the case of hematite), Fe(II) would be slowly generated (rate constant of 0.003 $M^{-1}$ $s^{-1}$ [57]) from reactions (5) (formation of a precursor surface complex of hydrogen peroxide) and (6) (electron transfer from ligand-to-metal within a surface complex). The surface lattice Fe(II) formed would react with hydrogen peroxide producing hydroxyl radicals (reaction (7)) initiating the oxidation reaction process. Peroxide radicals formed through reaction (6) (that dissociate through reaction (8)) may react with Fe(III) sites according to reaction (9). If both Fe(II) and Fe(III) are present (as in the case of magnetite) all the reactions (5)–(9) may take place.

After 150 min of contact time the following results were obtained: $q$ values of 0.26 and 0.81 mg $Fe_T$/g of hematite and magnetite ($7 \times 10^{-7}$ and $2.2 \times 10^{-6}$ M, respectively), 25–27% reduction of BPA concentrations and negligible hydrogen peroxide reduction in both cases. At the same experimental conditions and contact time but in the absence of hydrogen peroxide, negligible BPA adsorption over the iron oxides was noticed (<2%).

Previous studies on the catalytic decomposition of hydrogen peroxide on different iron oxides report that catalytic activity increases with the increasing iron oxide specific surface area [58,59]. However, in this work, the specific surface area of the iron oxides used was very small (23 and 28 $m^2$ $g^{-1}$ for hematite and magnetite, respectively) so as it is not expected a high activity. Thus, if reaction (6) is considered as the rate controlling step, the kinetics can be expressed through Eq. (10) [49]:

$$\frac{-\mathrm{d}[\mathrm{H_2O_2}]}{\mathrm{d}t} = k_1[\text{iron oxide}][\mathrm{H_2O_2}] \quad (10)$$

with hydrogen peroxide being consumed through the reduction of structural Fe(III) to Fe(II) (Eqs. (5) and (6)) and through the oxidation of Fe(II) (Eq. (7)).

In the case of hematite (no structural Fe(II)), hydrogen peroxide disappears through reactions (5) and (6), and through the oxidation of Fe(II) formed from (6) (Eq. (7)). Thus, starting with $5 \times 10^{-4}$ M initial concentration of hydrogen peroxide, considering a constant concentration of 0.15 g $L^{-1}$ hematite <> $1.88 \times 10^{-3}$ M Fe and assuming all Fe(II) formed undergoes fast oxidation to Fe(III) through reaction (7) [49,57], application of rate Eq. (10) would yield $3.4 \times 10^{-5}$ M after 150 min reaction, that is, maximum consumption of hydrogen peroxide would only be 7% of the initial concentration, which supports the negligible consumption of hydrogen peroxide experimentally observed. According to these reasoning only a fraction of this concentration would be used to remove the observed $2.5 \times 10^{-6}$ M of BPA.

Taking into account the low amount of iron leached, the results obtained would confirm the presence (magnetite) or formation (hematite) of Fe(II) on the oxide surface. This Fe(II) could react with hydrogen peroxide to generate hydroxyl radicals, actual oxidants of BPA.

### 3.1.6. Effect of UV-A radiation

As commented in Section 1, literature reports many examples on the positive effect of UV-A radiation to increase iron leaching from iron oxides through the photoreduction of surface Fe(III) to Fe(II). Photodissolution rate can be improved if Fe(III) carboxylates complexes (on the iron surface or in solution) able to photodecompose with a high quantum yield to form Fe(II) are formed. Because of the importance of this mechanism on the photocatalytic oxidation of contaminants in water, some iron leaching experiments were also carried out in the presence of UV-A radiation and carboxylic acids. Fig. 5a–d shows the results obtained when α-$Fe_2O_3$ and $Fe_3O_4$ were photoirradiated in the presence of tartaric and oxalic acids. From Fig. 5a and b it is observed that the presence of UV-A radiation increases the iron leaching process from α-$Fe_2O_3$ (this was also observed in the presence of citric and malic acids). In the case of $Fe_3O_4$ some similar effect is seen when tartaric (Fig. 5c), citric and malic acids (not shown) were present, but in the case of oxalic acid UV-A radiation has a positive effect on iron leaching only at the beginning of the process as observed from Fig. 5d. For the α-$Fe_2O_3$/carboxylic acids system the positive effect of UV-A radiation to increase iron leaching can be explained through the formation of Fe(III)–carboxylate (malate, citrate, tartrate or oxalate) complex that photoreduce to yield radicals and Fe(II) [7–10]. Fe(II) would act then as catalyst increasing the iron oxide dissolution rate. In the case of $Fe_3O_4$–carboxylic acids (different than oxalic acid) systems the positive effect of UV-A radiation was more pronounced. Iron leaching increased more than 3 times the values observed for α-$Fe_2O_3$. Thus, a similar explanation than above can be given in these cases. However, for the $Fe_3O_4$–oxalic acid system a significant inhibition of iron leaching is observed when UV-A radiation is applied after 3 h contact time (see Fig. 5d). In this system, the photochemistry of the ferrioxalate complex has to be dealt with, being the main reactions of this system in an acid medium as follows [60]:

$$[\mathrm{Fe(C_2O_3)_3}]^{3-} + h\nu \rightarrow \mathrm{Fe^{2+}} + 2\mathrm{C_2O_4^{2-}} + \mathrm{C_2O_4^{\bullet -}} \quad (11)$$

$$\mathrm{C_2O_4^{\bullet -}} \rightarrow \mathrm{CO_2^{\bullet -}} + \mathrm{CO_2} \quad (12)$$

$$\mathrm{CO_2^{\bullet -}} + \mathrm{O_2} \rightarrow \mathrm{CO_2} + \mathrm{O_2^{\bullet -}} \quad (13)$$

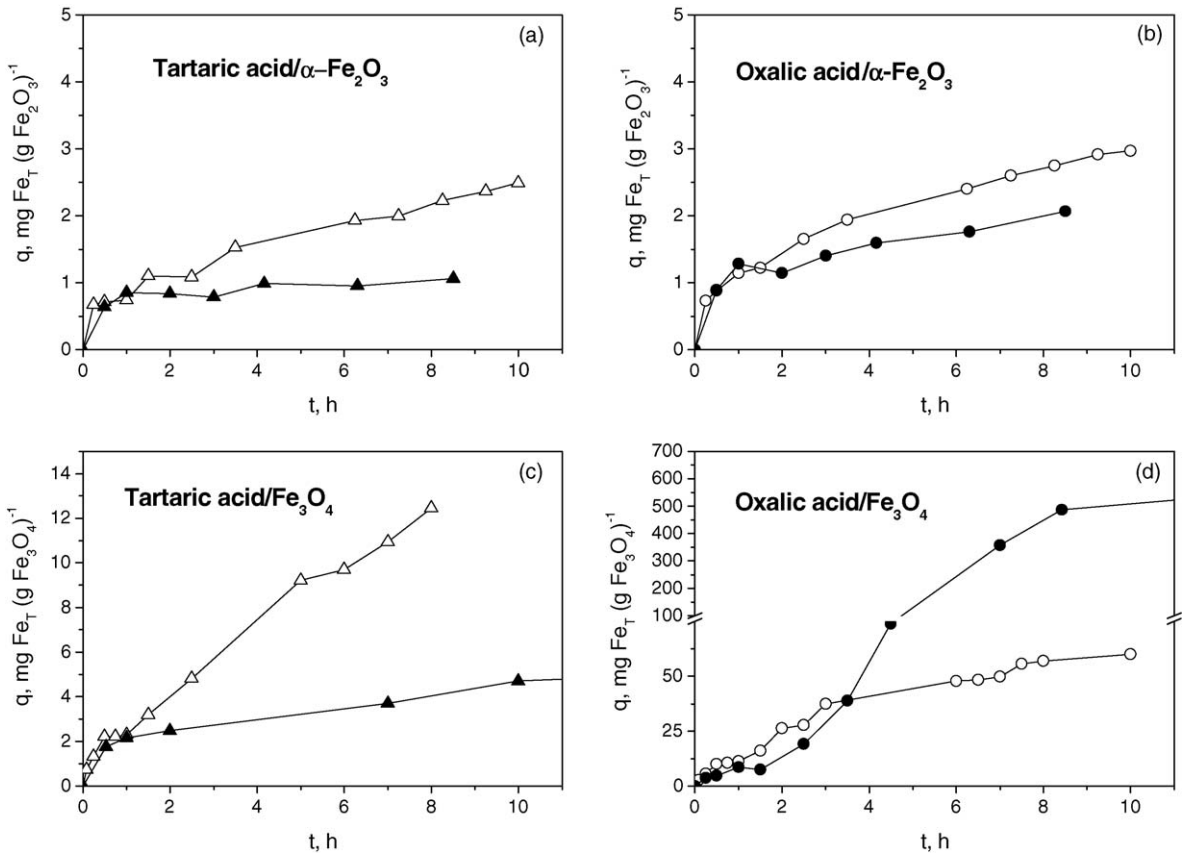


**Fig. 5.** Influence of UV-A radiation on $q$ changes with time for the $\alpha$-$Fe_2O_3$/carboxylic acid (up) and $Fe_3O_4$/carboxylic acid (down) systems. Experimental conditions: pH 3; 20 °C; [Iron oxide] = 0.15 g $L^{-1}$; agitation speed 800 rpm. Symbols (solid: in the dark; open: exposed to UV-A): ●, ○ [Oxalic acid]$_0$ = 0.01 M; ▲, △ [Tartaric acid]$_0$ = 0.01 M.

Thus, in the $Fe_3O_4$/oxalic acid/UV-A radiation system the ferrioxalate complex likely undergoes total photodecomposition into carbon dioxide, due to its high quantum yield (1.2 mol/einstein according to [43]). Then, the absence of oxalic acid would inhibit the leaching rate. TOC measurements after 8 and 10 h contact time confirmed this fact.

According to the results of iron oxide leaching at different experimental conditions, it can be concluded that oxalic acid is the most active carboxylic acid to promote iron dissolution from the iron oxides studied. This carboxylic acid was then applied in this work to compare different advanced oxidation systems involving UV-A radiation, iron oxides, titania and hydrogen peroxide to remove from water BPA, taken as model contaminant.

### *3.2. UV-A/iron oxide/oxalic acid oxidizing system to remove BPA from water*

The simultaneous presence of iron oxides, UV-A radiation and carboxylic acids is known to accelerate the degradation of organics in water [16–19]. The first step to study in these processes is to check the influence of direct photolysis. For the case of BPA this way of degradation does not develop when 365 nm UV-A radiation is used since BPA does not absorb UV radiation above 310 nm. However, the presence of oxalic acid and Fe(III) in water or on the iron oxide catalyst leads to ferrioxalate that rapidly photodecomposes with UV-A radiation through reactions (11)–(13). This can be deduced from Fig. 6 where the changes of normalized BPA remaining concentration (Fig. 6a and b) and amount of total iron leached per gram of iron oxide (Fig. 6c and d) with time corresponding to different advanced oxidation systems (UV-A/oxalic acid/iron oxide being one of them) are shown. From these results some conclusions can be deduced. Thus, iron leaching is an important step on the degradation of BPA as observed from experiments with hematite and magnetite. As shown in precedent sections, the amount of iron leached in the presence of oxalic acid from hematite was much lower than that from magnetite. Then, the higher BPA degradation rate observed in Fig. 6b when $Fe_3O_4$ is used is undoubtedly due to the higher amount of iron leached into the water from this iron oxide, as a result of the oxalic acid effect. In these experiments, after 120 min, total Fe dissolved in water was about 5.55 and 8.81 mg $g^{-1}$, for the case of hematite and magnetite, respectively, while 0.65 and 1.68 mg $g^{-1}$ of iron were leached in the absence of oxalic acid. Then, homogeneous photocatalytic oxidation plays a major role in treating water containing BPA.

In Fig. 6 the effect of the presence of titania is also shown. As it is observed from Fig. 6a, the UV-A/$\alpha$-$Fe_2O_3$/$TiO_2$ system allows higher BPA degradation rate than the UV-A/$TiO_2$ system, and the efficiency increases when oxalic acid is present. Thus, after 120 min BPA concentration was reduced 55%, 71% and 89% with the UV-A/$TiO_2$, UV-A/$\alpha$-$Fe_2O_3$/$TiO_2$ and UV-A/$\alpha$-$Fe_2O_3$/oxalic acid/$TiO_2$ systems, respectively. As reported in previous papers, the presence of some metal materials, such as iron oxide in this work, may reduce the energy gap of the titania semiconductor facilitating the migration of electrons from the valence band to the conduction band of titania and, hence, the formation rate of hydroxyl radicals. Another possible explanation may be due to the electron Fe(III) capturing effect that impedes the recombination between electrons and positive holes at the semiconductor surface [[57,61] and references there in]. In the presence of oxalic acid, the leaching rate from hematite increases and the Fe(III)–oxalate complex formed in water photoreduces yielding Fe(II) and radicals. In the presence of $TiO_2$, iron leaching could increase also from direct reduction of Fe(III) while capturing electrons of the

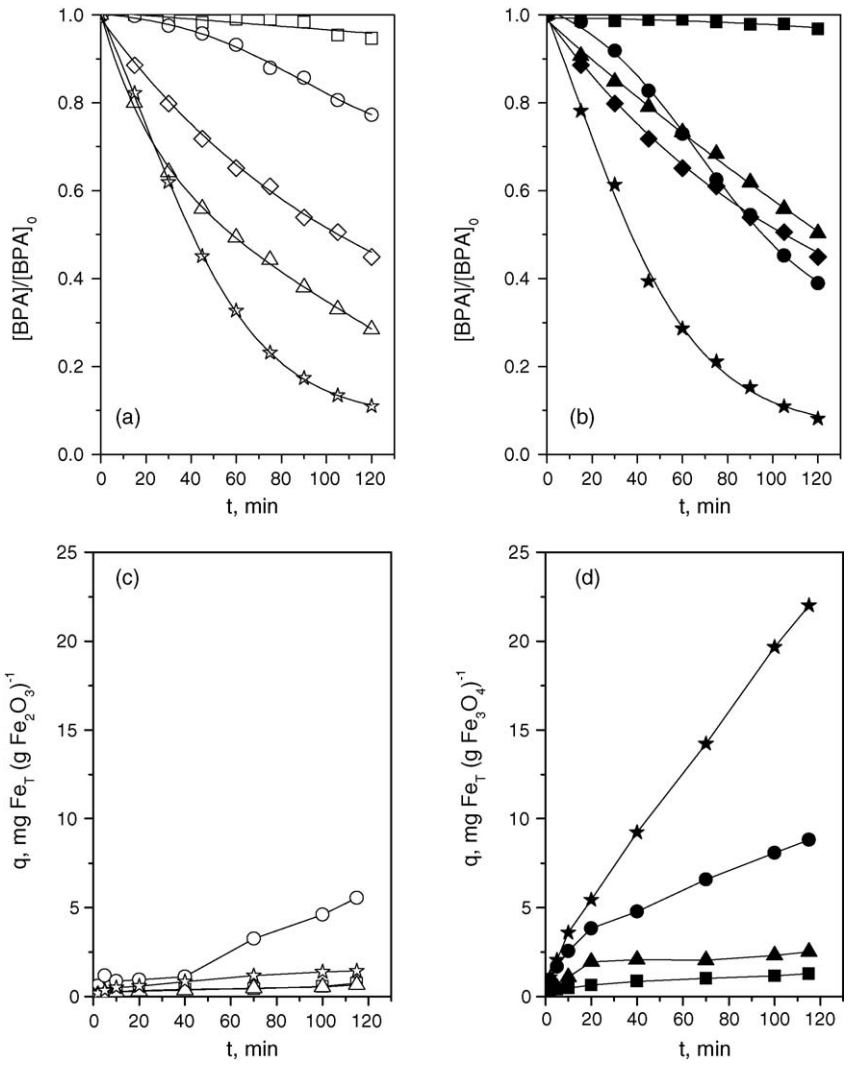


**Fig. 6.** Changes of remaining normalized BPA concentration (up) and $q$ (down) with irradiation time in the presence of α-$Fe_2O_3$ (open symbols) and $Fe_3O_4$ (solid symbols). Influence of $TiO_2$. Experimental conditions: $[BPA]_0 = 10^{-5}$ M; Initial concentration of iron oxide, $TiO_2$ and oxalic acid, when used, were: 0.15 g $L^{-1}$, 0.1 g $L^{-1}$ and $2 \times 10^{-4}$ M, respectively; $HClO_4/ClO_4^-$ pH 3, ionic strength: 0.03 M; $I_{365nm} = 7.33 \times 10^{-7}$ einstein $s^{-1}$; $T$ = 23–25 °C; Air bubbling. Symbols: □, ■, UV-A/iron oxide; ○, ● UV-A/iron oxide/oxalic acid; ◇, ◆ UV-A/$TiO_2$; △, ▲ UV-A/iron oxide/$TiO_2$; ☆, ★ UV-A/iron oxide/oxalic acid/$TiO_2$.

conduction band. However, as Fig. 6c shows, the amount of total iron leached after 120 min reaction when the UV-A/α-$Fe_2O_3$/oxalic acid/$TiO_2$ is applied (1.4 mg $g^{-1}$ < > $3.8 \times 10^{-6}$ M), is much lower than that observed from the application of the UV-A/α-$Fe_2O_3$/oxalic acid (5.5 mg $g^{-1}$ < > $1.48 \times 10^{-5}$ M) and slightly higher than that from UV-A/α-$Fe_2O_3$/$TiO_2$ (0.66 mg $g^{-1}$ < > $1.8 \times 10^{-6}$ M) system. These results suggest that hematite itself and Fe(III) in solution are the main responsible agents of BPA degradation by increasing $TiO_2$ photoactivity, with a minor contribution of ferrioxalate photoreduction.

Regarding magnetite, the changes of BPA remaining concentration and $q$ for the different oxidizing systems applied are shown in Fig. 6b and d, respectively. In this case, the presence of magnetite negatively affects the UV-A/$TiO_2$ system efficiency in removing BPA (Fig. 6b). According to the discussion on the hematite effects, by comparing the efficiency of UV-A/$TiO_2$ and UV-A/$Fe_3O_4$/$TiO_2$ systems on BPA degradation, the presence of magnetite does not improve the $TiO_2$ photocatalytic oxidation (that is, magnetite does not reduce the energy gap of the titania semiconductor nor avoid the $e^-$–$h^+$ recombination). Furthermore, the presence of magnetite would diminish the radiation path through the solution and, hence, the formation of hydroxyl radicals. Nonetheless, addition of oxalic acid to have the UV-A/$Fe_3O_4$/oxalic acid/$TiO_2$ system leads to a significant increase in BPA removal (92% after 120 min) and total iron leached (22 mg $g^{-1}$ < > $5.9 \times 10^{-5}$ M after 120 min, see also Fig. 6d). This suggests that, in this case, ferrioxalate photoreduction presents an important contribution to generate free radical species to eliminate BPA. Also, the amount of total iron leached after 120 min with the UV-A//$Fe_3O_4$/oxalic acid/$TiO_2$ system is much higher than that from UV-A/$Fe_3O_4$/oxalic acid (8.81 mg $g^{-1}$ < > $2.4 \times 10^{-5}$ M). Then, $TiO_2$ seems to favor the effect to dissolve iron from magnetite which could likely be due to reduction of dissolved Fe(III). The formed Fe(II), in its turn, would catalyze the leaching of iron oxide. This effect is also observed in the absence of oxalic acid. As it is shown in Fig. 6d, after 120 min reaction, $q$ values were 1.28 and 2.52 mg $g^{-1}$ when the UV-A/$Fe_3O_4$ and UV-A/$Fe_3O_4$/$TiO_2$ systems were applied, respectively. Notice that both the amount of iron leached and oxidation state have to be considered. Thus, if iron is only as Fe(II) (from Fe(III) photoreduction or Fe(III) reduction in the presence of $TiO_2$) it would not contribute to BPA degradation.

Since, on one hand, $Fe_3O_4$ does not seem to increase the $TiO_2$ action and, on the other hand, in the presence of oxalic acid Fe(III) and/or ferrioxalate are the main contributing agents to BPA

removal, the UV-A/$Fe_3O_4$/oxalic acid/$TiO_2$ system does not seem to be appropriate as a photocatalytic process given the high amount of iron leached. This leached iron should later be removed from water what would increase the capital, maintenance and operating costs of the process since a new coagulation/filtration unit would be needed. However, good results are now being obtained with this system at higher pH values when iron leaching from magnetite diminishes and photocatalytic activity of magnetite seems to increase. In addition, contrary to hematite, magnetite could be removed from water because of its magnetic properties.

Hydrogen peroxide is also known as an oxidant species that combined with iron and UV-A radiation form the Fenton and Photofenton processes. In a preceding Section 3.1.5, hydrogen peroxide was shown to decompose generating radicals at the iron oxide surface so that some heterogeneous Fenton or Photofenton (if UV-A radiation is also present) process develops. In this work, some other experiments were carried out in the presence of hydrogen peroxide as Fig. 7 shows.

For the case of hematite, Fig. 7a shows that the UV-A/α-$Fe_2O_3$/$H_2O_2$ process allows BPA degradation rates higher than the UV-A/$H_2O_2$, α-$Fe_2O_3$/$H_2O_2$ (dark) and UV-A/α-$Fe_2O_3$/oxalic acid systems. The amount of total iron leached with the UV-A/α-$Fe_2O_3$/$H_2O_2$ system was very low (0.3 mg $g^{-1}$ < > 8 × $10^{-7}$ M after 120 min) suggesting, on one hand, that Fenton reaction takes place on the iron oxide surface and, on the other hand, that UV-A radiation would favor Fenton reaction likely through surface Fe(III) photoreduction to yield Fe(II), that would instantaneously react with hydrogen peroxide to generate hydroxyl radicals and Fe(III) that, once more, would photoreduce to Fe(II) and so on. Furthermore, as it is observed from Fig. 7c, the total amount of iron leached was much lower than that leached from the UV-A/α-$Fe_2O_3$ system, which supports the low concentration of dissolved Fe observed. This is likely due to the fast reaction of hydrogen peroxide with Fe(II), formed from Fe(III) photoreduction, so that the remaining Fe(II) concentration is so low that negligible catalysis of iron leaching takes place. In the absence of light, since both hydrogen peroxide photolysis and Fe(III) photoreduction do not develop, only Fe(II) on the iron oxide surface or formed through reactions (6) and (7) is the responsible agent of BPA degradation.

For the case of magnetite, Fig. 7b shows that the UV-A/$Fe_3O_4$/$H_2O_2$ process allow BPA degradation rates higher than that obtained by the UV-A/$H_2O_2$ and the $Fe_3O_4$/$H_2O_2$ (dark) systems, while the total iron leached (Fig. 7d) was similar to that obtained in the absence of light. According to these results, comparing the efficacy of the Fenton and Photofenton systems and taking into

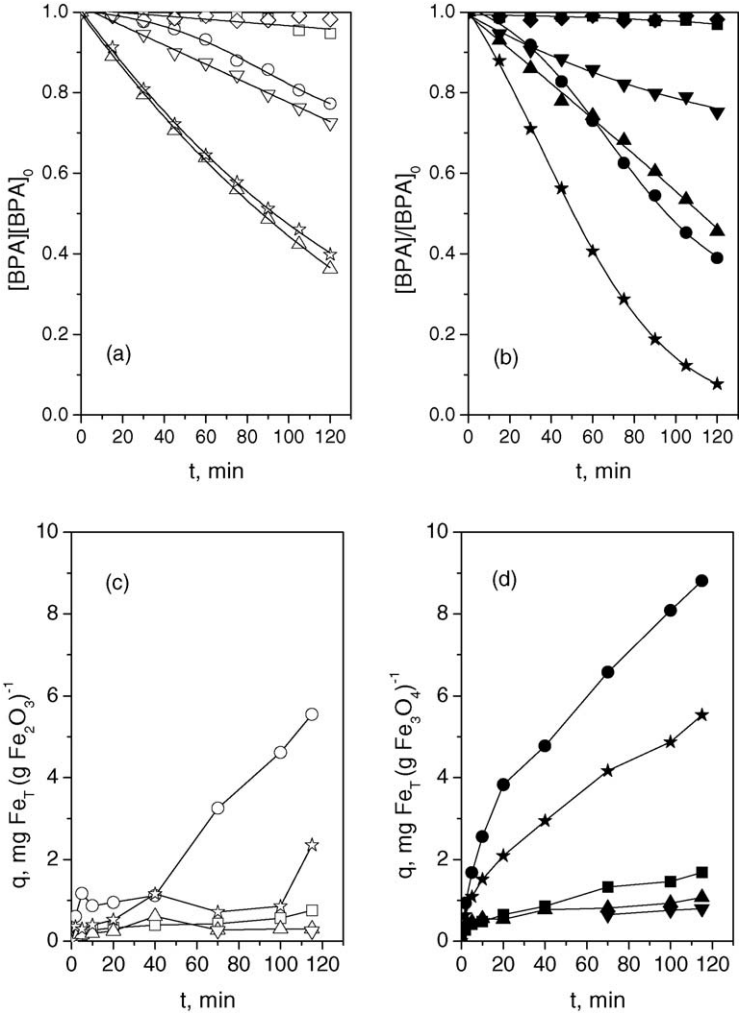


**Fig. 7.** Changes of remaining normalized BPA concentration (up) and $q$ (down) with irradiation time in the presence of α-$Fe_2O_3$ (open symbols) and $Fe_3O_4$ (solid symbols). Influence of hydrogen peroxide. Experimental conditions: $[BPA]_0 = 10^{-5}$ M; Initial concentration of iron oxide, hydrogen peroxide and oxalic acid, when used, were: 0.15 g $L^{-1}$, 5 × $10^{-4}$ M and 2 × $10^{-4}$ M, respectively; $HClO_4/ClO_4^-$ pH 3, ionic strength: 0.03 M; $I_{365nm}$ = 7.33 × $10^{-7}$ einstein $s^{-1}$; $T$ = 23–25 °C; Air bubbling. Symbols: □, ■, UV-A/iron oxide; ○, ● UV-A/iron oxide/oxalic acid; ◇, ◆ UV-A/$H_2O_2$; △, ▲ UV-A/iron oxide/$H_2O_2$; ▽, ▼ iron oxide/$H_2O_2$ (dark); ☆, ★ UV-A/iron oxide/oxalic acid/$H_2O_2$.

**Table 1**
BPA degraded, total iron leached and hydrogen peroxide consumed after 120 min for the different processes tested[a].

| Process | [BPA] degraded (%) | $Fe_T$ (mg $g^{-1}$) | [$H_2O_2$] consumed (%) |
|---|---|---|---|
| UV-A/$Fe_3O_4$/oxalic acid/$TiO_2$/$H_2O_2$ | 100 ($t_{1/2}$ 10 min)[a] | 9.22 | 68.7 |
| UV-A/α-$Fe_2O_3$/oxalic acid/$TiO_2$/$H_2O_2$ | 100 ($t_{1/2}$ 15 min)[a] | 1.15 | 49.4 |
| UV-A/$Fe_3O_4$/$TiO_2$/$H_2O_2$ | 100 ($t_{1/2}$ 18 min)[a] | 1.43 | 77.5 |
| UV-A/α-$Fe_2O_3$/$TiO_2$/$H_2O_2$ | 100 ($t_{1/2}$ 24 min)[a] | 0.52 | 46.7 |
| UV-A/$Fe_3O_4$/oxalic acid/$H_2O_2$ | 92.3 | 5.53 | <5 |
| UV-A/$Fe_3O_4$/oxalic acid/$TiO_2$ | 91.9 | 22.0 | – |
| UV-A/α-$Fe_2O_3$/oxalic acid/$TiO_2$ | 89.0 | 1.43 | – |
| UV-A/α-$Fe_2O_3$/$TiO_2$ | 71.5 | 0.66 | – |
| UV-A/$TiO_2$/$H_2O_2$ | 67.7 | – | 49.1 |
| UV-A/α-$Fe_2O_3$/$H_2O_2$ | 63.7 | 0.30 | <5 |
| UV-A/$Fe_3O_4$/oxalic acid | 61.0 | 8.81 | – |
| UV-A/α-$Fe_2O_3$/oxalic/$H_2O_2$ | 60.2 | 2.35 | <5 |
| UV-A/$TiO_2$ | 56.4 | – | – |
| UV-A/$Fe_3O_4$/$H_2O_2$ | 54.4 | 1.07 | <5 |
| UV-A/$Fe_3O_4$/$TiO_2$ | 50.3 | 2.52 | – |
| α-$Fe_2O_3$/$H_2O_2$ (dark) | 27.5 | 0.25 | <5 |
| UV-A/$H_2O_2$ | <2 | – | <5 |
| $Fe_3O_4$/$H_2O_2$ (dark) | 24.8 | 0.80 | <5 |
| UV-A/α-$Fe_2O_3$/oxalic acid | 22.7 | 5.55 | – |
| UV-A/α-$Fe_2O_3$ | <5 | 0.75 | – |
| UV-A/$Fe_3O_4$ | <5 | 1.28 | – |
| $H_2O_2$ (dark) | <2 | – | <5 |

Experimental conditions: $[BPA]_0 = 10^{-5}$ M; [Iron oxide]: 0.15 g $L^{-1}$; $[H_2O_2]_0 = 5 \times 10^{-4}$ M; [$TiO_2$] = 0.1 g $L^{-1}$; [Oxalic acid]$_0 = 2 \times 10^{-4}$ M; $HClO_4/ClO_4^-$ pH 3, ionic strength: 0.03 M; $I_{365nm} = 7.33 \times 10^{-7}$ einstein $s^{-1}$; $T$ = 23–25 °C; Air bubbling.

[a] Fitted to pseudo-first order kinetics. In all cases $R^2 > 0.99$.

account the presence of structural Fe(II) in magnetite, Fe(II) formed through Fe(III) photoreduction rather than structural Fe(II) seems to be the main species involved in BPA degradation. On the other hand, Fe(II) dissolved concentration keeps too low to catalyze the iron leaching process since Fe(II)–hydrogen peroxide reaction is very fast.

By comparing the efficiency of UV-A/α-$Fe_2O_3$/$H_2O_2$ and UV-A/$Fe_3O_4$/$H_2O_2$ systems to remove BPA (see Fig. 7a and b, up triangles), the rate of oxidation when hematite is present (64% BPA removed after 120 min) is higher than that in the presence of magnetite (55% BPA removed after 120 min). Once more, the results suggest Fe(II) formed at the iron surface through the Fe(III) photoreduction rather than the structural Fe(II) as the main species involved in the heterogeneous Fenton process.

Contrarily to what has been observed in the case of hematite, addition of oxalic acid to the UV-A/$Fe_3O_4$/$H_2O_2$ system gives rise to a significant increase in process efficiency with 90% BPA conversion in 120 min. In this experiment, the total amount of iron leached was also higher (5.53 mg $g^{-1}$ $<>$ $1.5 \times 10^{-5}$ M) though lower than that from the UV-A/$Fe_3O_4$/oxalic acid system application. Then, in addition to heterogeneous Fenton reaction and Fe(III) photoreduction, formation of hydroxyl radical species through ferrioxalate photolysis and homogeneous Fenton reaction become mechanisms to be considered.

Negligible decrease in hydrogen peroxide concentration was noticed in all the experiments with added hydrogen peroxide (see Table 1, runs in the absence of $TiO_2$).

Finally, a last series of BPA oxidation experiments involving all of the reagents used (UV-A/$TiO_2$/$H_2O_2$, UV-A/iron oxides/$TiO_2$/$H_2O_2$ and UV-A/iron oxides/oxalic acid/$TiO_2$/$H_2O_2$) was carried out. By fitting experimental BPA–time curves to pseudo-first order kinetics BPA half lives of 10–15 min were observed for UV-A/iron oxides/oxalic acid/$TiO_2$/$H_2O_2$ systems that favorably compare to those of the previous systems studied (see Table 1 for all values). These results are undoubtedly due to the multiple ways of hydroxyl radical formation when all reagents studied are simultaneously applied. Decision regarding the best system will depend on high BPA removal efficiency, low iron leaching and hydrogen peroxide consumption to generate oxidant species.

## 4. Conclusions

Main conclusions reached in this work are:

For iron leaching study:

Among carboxylic acids studied, oxalic acid was found as the most active to dissolve iron from any of the iron oxides used. However, leaching from magnetite was more efficient than that from hematite.

The ratio carboxylic acid/iron oxide, concentration of protons, contact time and temperature, all of them exert positive effects on iron leaching.

Regardless of temperature and carboxylic acid presence, when hematite was used iron leaching process was chemically controlled.

Regarding magnetite, iron leaching was also chemically controlled at 20 °C except for oxalic acid, while at temperatures >20 °C mass transfer was slow step except for citric and malic acids.

UV-A radiation also favors iron leaching regardless of the nature of iron oxide.

For BPA oxidation:

Application of UV-A/iron oxide/oxalic acid/$H_2O_2$/$TiO_2$ system allows total consumption of BPA in less than 120 min with half life lower than 15 min.

Different mechanisms of oxidation: Fenton (homogeneous and heterogeneous), Photofenton, ferricarboxylate photodecomposition and oxidation through positive holes contribute to BPA degradation in this complete oxidizing system.

Regardless of the system applied, hematite presents a higher stability than magnetite.

New studies on the pH effect and solar light application as UV-A source to improve the efficiency of the oxidizing systems present in this work are now in progress and will be the subject of future reports.

## Acknowledgment

Authors thank Junta de Extremadura and European Social Funds (Research project: PRI07C066) for the economic support.

## References

[1] O.A. Jones, J.N. Lester, N. Voulvoulis, Trends Biotechnol. 23 (2005) 163–167.
[2] W.H. Glaze, J.W. Kang, D.H. Chapin, Ozone Sci. Eng. 9 (1987) 335–342.
[3] M.I. Litter, Appl. Catal. B: Environ. 23 (1999) 89–114.
[4] D.S. Bhatkhande, V.G. Pasngarkar, A.C.M. Beenackers, J. Chem. Technol. Biotechnol. 77 (2001) 102–116.
[5] S. Yurdakal, V. Loddo, V. Augugliaro, H. Berber, G. Palmisano, L. Palmesano, Catal. Today 129 (2007) 9–15.
[6] F. Méndez-Arriaga, S. Esplugas, J. Giménez, Water Res. 43 (2008) 585–594.
[7] M.I. Litter, M.A. Blesa, Can. J. Chem. 70 (1992) 2502–2510.
[8] A. Safarzadeh-Amiri, J. Bolton, S. Cater, Water Res. 31 (1997) 787–798.
[9] M.I. Franch, J.A. Ayllón, J. Peral, X. Doménech, Appl. Catal. 50 (2004) 89–99.
[10] E.M. Rodríguez, B. Núñez, G. Fernández, F.J. Beltrán, Appl. Catal. B: Environ. 89 (2009) 214–222.
[11] N. Deng, F. Wu, F. Luo, M. Xiao, Chemosphere 36 (1998) 3101–3112.
[12] W. Feng, D. Nansheng, Z. Yuegang, Chemosphere 39 (1999) 2079–2085.
[13] L. Wang, C.B. Zhang, F. Wu, N.S. Deng, J. Coord. Chem. 59 (2006) 803–813.
[14] Y. Chen, F. Wu, Y. Lin, N. Deng, N. Bazhin, E. Glebov, J. Hazard. Mater. 148 (2007) 360–365.
[15] C. Decoret, J. Royer, B. Legube, M. Doré, Environ. Technol. Lett. 5 (1984) 207–218.
[16] F.B. Li, X.Z. Li, X.M. Li, T.X. Liu, J. Dong, J. Colloid Interface Sci. 311 (2007) 481–490.
[17] F.B. Li, X.Z. Li, C.S. Liu, X.M. Li, T.X. Liu, Ind. Eng. Chem. Res. 46 (2007) 781–787.
[18] X. Wang, C. Liu, X. Li, F. Li, S. Zhou, J. Hazard. Mater. 153 (2008) 426–433.
[19] Q. Lan, F. Li, C. Liu, X.Z. Li, Environ. Sci. Technol. 42 (2008) 7918–7923.

[20] M.A. Blesa, P.J. Morando, A.E. Regazzoni, Chemical Dissolution of Metal Oxides, CRC Press, Boca Raton, FL, 1994, pp. 269–308.
[21] R.M. Cornell, U. Schwertmann, The Iron Oxides: Structure, Properties, Reactions, Occurrences and Uses, 2nd Ed., Wiley-VCH Verlag GmbH & Co. KGaA, Weinheim, 2003.
[22] B. Zinder, G. Furrer, W. Stumm, Geochim. Cosmochim. Acta 50 (1986) 1861–1869.
[23] D. Panias, M. Taxiarchou, I. Douni, I. Paspaliaris, A. Kontopoulos, Hydrometallurgy 43 (1996) 219–230.
[24] M. Taxiarchou, D. Panias, I. Douni, I. Paspaliaris, A. Kontopoulos, Hydrometallurgy 44 (1997) 287–299.
[25] P.S. Sidhu, R.J. Gilkes, R.M. Cornell, A.M. Posner, J.P. Quirk, Clays Clay Miner. 29 (1981) 269–276.
[26] B.C. Faust, M.R. Hoffmann, Environ. Sci. Technol. 20 (1986) 943–948.
[27] M.I. Litter, M.A. Blesa, J. Colloid Interface Sci. 125 (1988) 679–687.
[28] C. Siffert, B. Sulzberger, Langmuir 7 (1991) 1627–1634.
[29] S.O. Pehkonen, R. Siefert, Y. Erel, S. Webb, M.R. Hoffmann, Environ. Sci. Technol. 27 (1993) 2056–2062.
[30] M.I. Litter, M. Villegas, M.A. Blesa, Can. J. Chem. 72 (1994) 2037–2043.
[31] C. Guillard, C.F. Hoang-Van, P. Pichat, F. Marme, J. Photochem. Photobiol. A: Chem. 89 (1995) 221–227.
[32] S.O. Pehkonen, R.L. Siefert, M.R. Hoffmann, Environ. Sci. Technol. 29 (1995) 1215–1222.
[33] B. Sulzberger, H. Laubscher, Mar. Chem. 50 (1995) 103–115.
[34] P.M. Borer, B. Sulzberger, P. Reichard, S.M. Kraemer, Mar. Chem. 93 (2005) 179–193.
[35] T.D. Waite, F.M.M. Morel, J. Colloid Interface Sci 102 (1984) 121–137.
[36] T. Yamamoto, A. Yasuhara, H. Shiraishi, O. Nakasugi, Chemosphere 42 (2001) 415–418.
[37] I. Gültekin, N.H. Ince, J. Environ. Manage. 85 (2007) 816–832.
[38] L.L. Stookey, Anal. Chem. 42 (1970) 779–781.
[39] E.M. Rodríguez, M. Mimbrero, F.J. Masa, F.J. Beltrán, Water Res. 41 (2007) 1325–1333.
[40] Y. Zuo, J. Hazard. Mater. Acta 59 (1995) 3123–3130.
[41] G.M. Eisenberg, Ind. Eng. Chem. 15 (1943) 327–328.
[42] W. Maschelein, M. Denis, R. Ledent, Water Sewage Works 32 (1977) 69–72.
[43] C.G. Hatchard, C.A. Parker, Proc. R. Soc. London, Ser. A 235 (1956) 518–536.
[44] R. Chiarizia, E.P. Horwitz, Hydrometallurgy 27 (1991) 339–360.
[45] V.R. Ambikadevi, M. Lalithambika, Appl. Clay Sci. 16 (2000) 133–145.
[46] Y. Zhang, N. Kallay, E. Matijevicy, Langmuir 1 (1985) 201–206.
[47] N. Xu, Y. Gao, Appl. Geochem. 23 (2008) 783–793.
[48] H.J.H. Fenton, Chem. News 33 (1876) 190.
[49] S.S. Lin, M.D. Gurol, Environ. Sci. Technol. 32 (1998) 1417–1423.
[50] H.H. Huang, M.C. Lu, J.N. Chen, Water Res. 35 (2001) 2291–2299.
[51] A.M. Teel, C.R. Warberg, D.A. Atkinson, R.J. Watts, Water Res. 35 (2001) 977–984.
[52] W.P. Kwan, B.M. Voelker, Environ. Sci. Technol. 37 (2003) 1150–1158.
[53] P. Baldrian, V. Merhautová, J. Gabriel, F. Nerud, P. Stopka, M. Hrubý, M.J. Benes, Appl. Catal. B: Environ. 66 (2006) 258–264.
[54] M. Hermanek, R. Zboril, I. medrik, J. Pechousek, C. Gregor, J. Am. Chem. Soc. 129 (2007) 10929–10936.
[55] R. Matta, K. Hanna, S. Chiron, Sci. Total Environ. 385 (2007) 242–251.
[56] X. Xue, K. Hanna, N. Deng, J. Hazard. Mater. 166 (2009) 432–440.
[57] F. Mazille, T. Schoettl, C. Pulgarín, Appl. Catal. B Environ. 89 (2009) 635–644.
[58] R.L. Valentine, H. Wang, J. Environ. Eng. 131 (1998) 31–38.
[59] H.H. Huang, M.C. Lu, J.N. Chen, Water Res. 9 (2001) 2291–2299.
[60] V. Balzani, V. Carassiti, Photochemistry of Coordination Compounds, Academic Press, London, 1970.
[61] F. Mazille, A. López, C. Pulgarín, Appl. Catal. B Environ. 90 (2009) 321–329.